Recrystallization and Superplasticity at 300 °C in an Aluminum-Magnesium Alloy

S.J. HALES, T.R. McNELLEY, and H.J. McQUEEN

Variations in thermomechanical processing (TMP) which regulate the microstructural characteristics and superplastic response of an Al-10Mg-0.1Zr alloy at 300 °C were evaluated. Mechanical property data revealed that the superplastic ductility can be enhanced by simultaneously increasing the total rolling strain, the reduction per pass, and the duration of reheating intervals between passes during isothermal rolling. Texture and microscopy data were consistent with the development of a refined microstructure by recovery-dominated processes, *i.e.*, continuous recrystallization, during the processing. The mechanisms by which a refined substructure can be progressively converted into a fine-grained structure during repeated cycles of deformation and annealing are addressed. A qualitative description of the complex sequence of developments leading to a microstructure better suited to support superplastic response is presented.

I. INTRODUCTION

INVESTIGATIONS into fine-grained superplasticity in Al-Cu-Zr (Supral) alloys have shown that the development of refined microstructures occurs by continuous recrystallization (CRX) during tensile deformation.[1–6] In these studies, the thermomechanical processing (TMP) was designed to produce an essentially unrecrystallized condition. At the onset of subsequent tensile deformation, a well-defined substructure was stabilized by fine second-phase precipitates. An increase in the strain-rate sensitivity coefficient, m, during the early stages of deformation was correlated with the occurrence of strain-induced dynamic CRX.[4] The initial transient in m value was assumed to result from the development of a fine-grained microstructure during straining and a shift to superplastic deformation mechanisms. The texture present at the conclusion of the TMP exhibited characteristic components of deformed, unrecrystallized material. These components gradually weakened as a result of the random grain rotations associated with superplastic deformation mechanisms, and no new texture components appeared.[6]

Previous work on warm-rolled Al-Mg-X alloys containing 6 to 10 wt pct Mg has also indicated that refined grain structures and superplastic ductility can be produced by CRX.[7–12] In contrast to similarly processed Al-Cu-Zr alloys, however, the apparent m value decreased during uniaxial deformation at 300 °C.[9] Subsequent transmission electron microscopy (TEM) studies have revealed that the misorientations of the constituent boundaries are distributed from 2 to 15 deg initially and increase to 10 to 30 deg after 100 pct tensile elongation.[10] It was proposed that the microstructure was already capable of sustaining superplastic deformation mechanisms at the onset of uniaxial testing.[11] Consequently, the decrease in apparent m value was assumed to be a result of strain-induced grain growth during deformation. However, it has remained uncertain as to whether the boundaries created by the alternate warm rolling and static annealing of the TMP should be described as recovered subboundaries or as continuously recrystallized grain boundaries.[12]

Continuous recrystallization is generally considered to be a recovery-dominated process resulting in a progressive increase in boundary misorientation and conversion of low-angle boundaries into higher angle boundaries. The microstructure must be stabilized by particles, and its evolution is often the result of a combined precipitation/recrystallization reaction which occurs under both static and dynamic conditions.[13–16] Current understanding of the mechanism of static CRX during annealing of cold-worked metastable solid solutions is summarized in the schematic of Figure 1. Dynamic CRX during tensile elongation occurs in a similar but more rapid manner, since these mechanisms are aided by applied stress.[1,17]

The premise for this study was that it is possible to generate a refined structure consisting of a sufficient areal fraction of grain boundaries to support superplastic deformation mechanisms at the conclusion of TMP itself. The structural transformations involved occur progressively during alternate cycles of warm rolling and static annealing. Depending on the processing schedule, such structures may exhibit varying degrees of static and dynamic CRX during the TMP and additional CRX, followed by grain rotation and coarsening, during superplastic deformation.

II. EXPERIMENTAL PROCEDURE

The composition of the alloy studied is given in Table I. The eutectic temperature is 451 °C, and the principal second phase is β (Al_8Mg_5), which has a solvus temperature of ≈365 °C.[18] The various TMP schedules employed to assess the effect of rolling parameters on superplastic ductility are summarized in Figure 2. In all cases, the material was initially solution treated and hot

S.J. HALES, Research Engineer, is with Analytical Services and Materials, Inc., NASA Langley Research Center, Hampton, VA 23665-5225. T.R. McNELLEY, Professor, is with the Department of Mechanical Engineering, Naval Postgraduate School, Monterey, CA 93943-5000. H.J. McQUEEN, Professor, is with the Mechanical Engineering Department, Concordia University, Montreal, PQ H3G 1M8, Canada.

Manuscript submitted September 15, 1989.

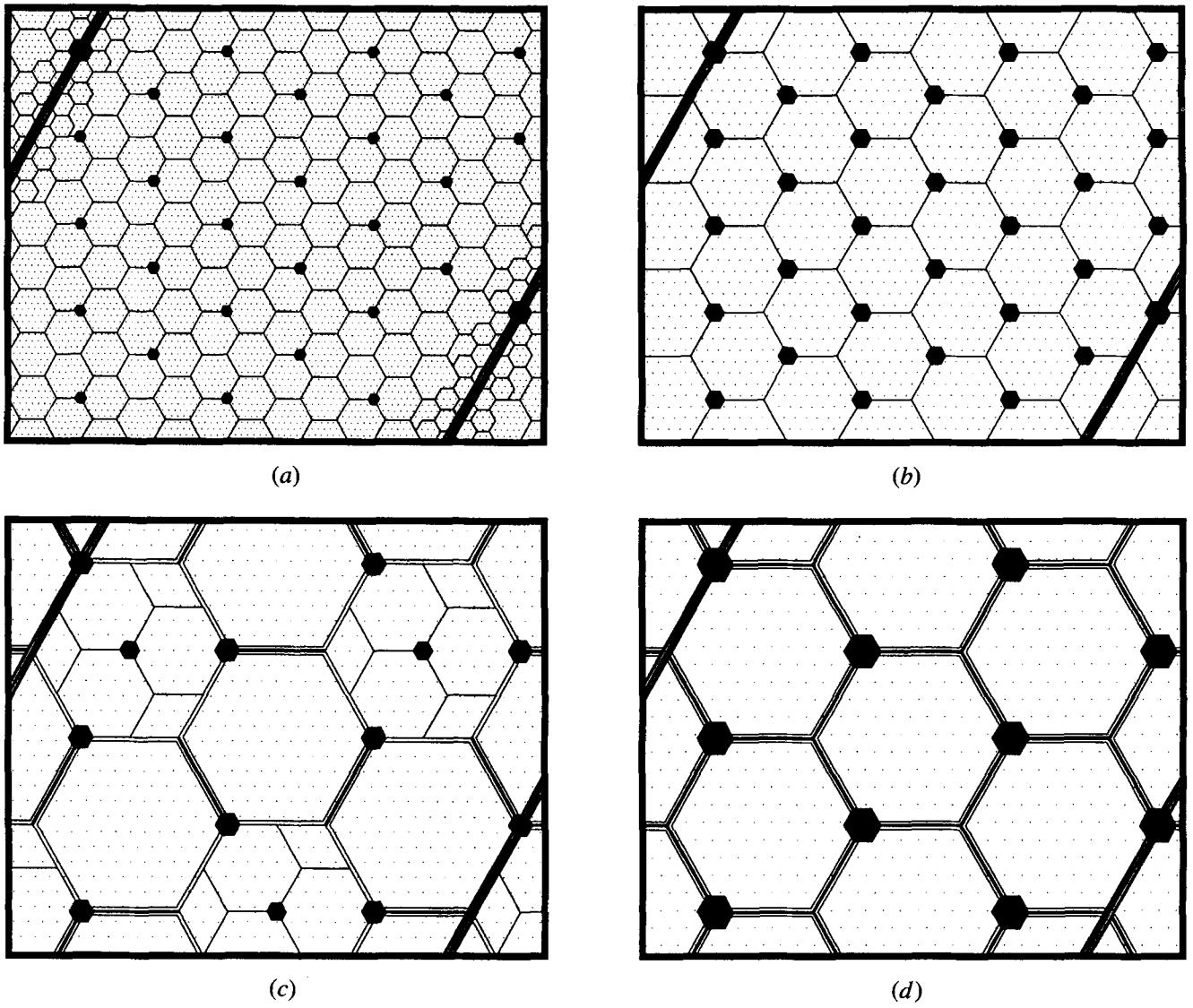

Fig. 1—A summation of the current understanding of static continuous recrystallization of a heavily cold-worked structure. The reaction relies on the existence of a homogeneous distribution of strain in the deformed microstructure with no intensified zones adjacent to large particles. The sequence of events is as follows: (a) polygonization by mutual annihilation and migration of dislocations to form a network of walls; (*b*) coarsening of the network to form a well-defined substructure stabilized by second-phase precipitates; (*c*) subgrain growth by rotation and coalescence in conjunction with particle coarsening; and (*d*) a progressive increase in misorientation to boundaries which are moderate- to high-angle in character.

Table I. Alloy Composition (Weight Percent)

Mg	Zr	Si	Fe	Ti	Be	Al
9.89	0.09	0.02	0.02	0.01	0.0003	bal.

forged at 440 °C to homogenize the microstructure. Subsequently, warm rolling was conducted at 300 °C for the majority of the processing. The equilibrium volume fraction of the β phase is 10 pct at 300 °C, based on published phase diagram data.[18] Two additional rolling temperatures, 220 °C and 350 °C, were selected to assess the effect of temperature during processing.

Approximately isothermal conditions were maintained by including reheating intervals between consecutive rolling passes. A constant reduction per pass resulted in a progressive increase in the average strain rate through the rolling sequence. The average strain rate during rolling increased from $\approx 10^0$ s^{-1} for the initial pass to $\approx 10^1$ s^{-1} for the final pass, depending on the specific TMP schedule employed. The total strain accumulated during rolling was calculated from the reduction in area as $\ln (A_0/A_f)$, where A_0 and A_f are the initial and final cross-sectional areas of the billet, respectively.

Details of the TMP schedules are presented in Table II and show how the effect of specific variables on superplastic ductility may be isolated. This study is an extension of earlier work which included only the combination

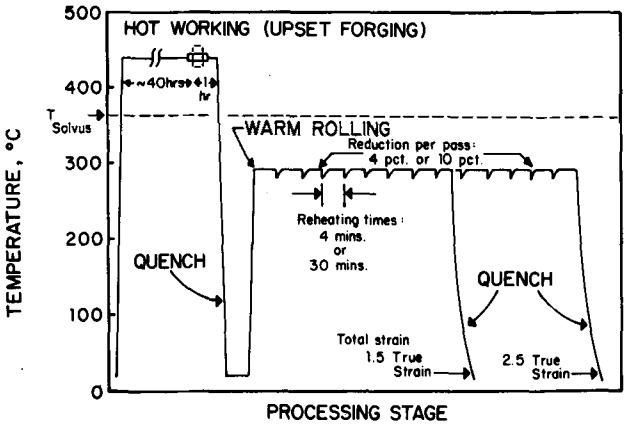

Fig. 2—Schematic representation of the TMP method employed; specific combinations of the processing variables are summarized in Table II to allow comparison of the specific effects.

Table II. Thermomechanical Processing Schedules

TMP Schedule	Fixed Reduction Per Pass (Pct)	Reheating Time between Passes (Min)	Total True Strain
I	4	4	1.5
II	10	4	1.5
III	4	4	2.5
IV	4	30	2.5
V	10	4	2.5
VI	10	30	2.5

of processing parameters designated as TMP III. These schedules were selected initially based on the limitations of the existing laboratory-scale facilities.[10]

Tension testing was conducted at 300 °C ± 2 °C, corresponding to a homologous temperature of $0.6T_m$, on samples prepared with tensile axes parallel to the rolling direction. Samples required 45 minutes to equilibrate at the test temperature prior to initiation of straining. Tests were conducted to failure using constant crosshead speeds, and nominal strain rates varied from 6.7×10^{-5} s^{-1} to 1.7×10^{-1} s^{-1}. The load *vs* time data were reduced to true stress *vs* true strain curves, and subsequent plots of flow stress *vs* strain rate were compensated for the decrease in true strain rate with increasing strain.[9]

Pole figure data were collected to assess behavior in this alloy in comparison to previous work citing CRX as the mechanism of microstructural evolution.[6] Texture analyses were performed on material processed by TMP III. Samples were extracted from the as-rolled material and from the grip and gage sections of tensile specimens strained to 100 pct elongation at a strain rate of 1.7×10^{-2} s^{-1}. In each case, the surface analyzed corresponded to the midplane of bulk material. Digitized intensity data, collected using a high precision goniometer, were reduced to the corresponding {111} or {200} pole figures extending out to ≈70 deg to the sheet normal.

The degree of microstructural coarsening occurring during tensile deformation was evaluated through TEM of either the grip or the gage sections of tensile samples from material processed using the various TMP schedules. Specimens were prepared in the plane of the sheet and were examined by conventional methods in a JEOL 100CX microscope operating at 120 kV. Grip material from tensile specimens tested at the highest strain rate, at which failure occurred within 15 seconds, corresponded closely to the preheating time prior to testing. Gage sections were examined for specimens deformed at the strain rate at which peak ductilities were obtained for each processing condition. Conventional bright-field imaging of several locations, in conjunction with multiple foil orientations, was used to ensure observation of all boundaries.

III. RESULTS

A. *Mechanical Properties*

1. *Total rolling strain (TMP I vs TMP III)*

True rolling strains of 1.5 and 2.5, corresponding to ≈78 pct and ≈92 pct reduction in area, were chosen to assess the effect of total rolling strain on superplastic ductility. The mechanical property data in Figure 3(a) show that there is a significant change in behavior on increasing the rolling strain. The flow stress for TMP III material is less at all strain rates, and the sigmoidal curve has a longer region with maximum slope. The corresponding maximum m value (≈0.4) is at a strain rate of 6.7×10^{-3} s^{-1} and coincides with the peak ductility of 450 pct. The material which has experienced the lesser rolling strain, TMP I, exhibits a peak ductility of only 170 pct and at a lower strain rate. The enhancement of the superplastic response by an increase in the amount of rolling deformation of this material is essentially the same as a result reported earlier for an Al-8Mg-0.5Li-0.2Zr alloy.[19]

2. *Reduction per rolling pass (TMP III vs TMP V and TMP IV vs TMP VI)*

Upon consideration of the improvement in superplastic ductility achieved by increasing the total rolling strain, it was anticipated that a more severe reduction per rolling pass, also producing a higher dislocation density, would have a similar effect. However, comparison of data for materials processed using a 4-minute reheating interval, namely, TMP III *vs* TMP V, reveals that increased reduction per rolling pass drastically reduced the subsequent peak ductility, from 450 pct to 250 pct. The change in rolling schedule also resulted in less total time accumulated at the rolling temperature and thus less recovery and precipitation. Given the contribution of these to the process of continuous recrystallization, it was surmised that a longer reheating interval between rolling passes would lead to the desired microstructural evolution.

The results of increasing the reduction from 4 to 10 pct with a 30-minute reheating interval between rolling passes are presented in Figure 3(b). For the TMP VI material, with larger reduction per pass compared to the TMP IV material, the flow stress has been reduced approximately 40 pct and the ductility increased from ≈475 pct to ≈600 pct at a strain rate of 1.7×10^{-3} s^{-1}. These data indicate that increasing the dislocation density in each rolling step aids in the development of a superplastic, fine-grained microstructure, but only if accompanied by increased reheating time between passes.

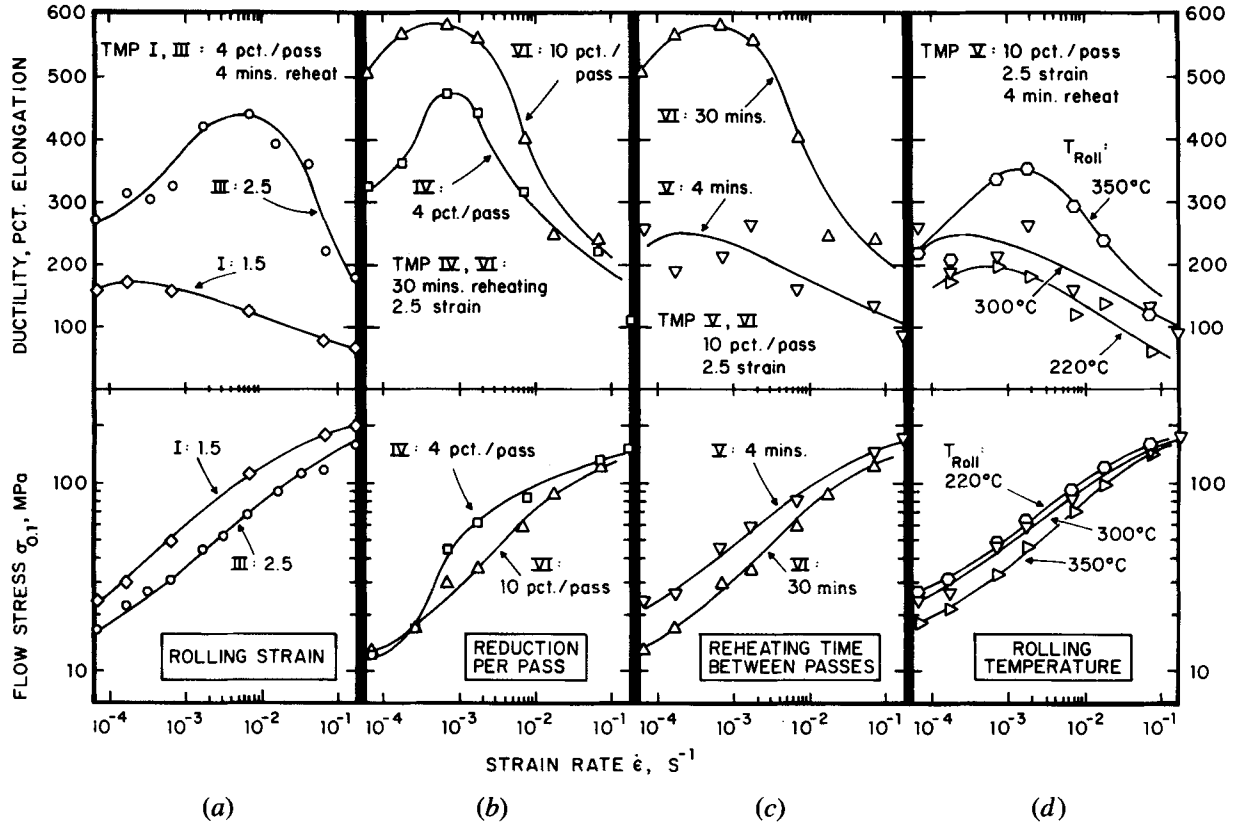

Fig. 3—Mechanical property data illustrating the effect of variation in TMP on superplastic response at 300 °C: (*a*) total rolling strain, (*b*) reduction per rolling pass, (*c*) reheating time between rolling passes, and (*d*) rolling temperature.

3. *Reheating time between rolling passes (TMP V vs TMP VI)*

Data illustrating the difference in superplastic behavior between material rolled with 4- and 30-minute reheating times between passes are shown in Figure 3(c): there is a dramatic increase in ductility, from ≈250 pct for TMP V to ≈600 pct for TMP VI at a strain rate of 1.7×10^{-3} s^{-1}. The flow stress has decreased by 20 to 40 pct for all strain rates, with an increase in the maximum slope to $m \approx 0.5$, which is commonly associated with grain-boundary sliding as the predominant deformation mechanism. It is clear that a large strain per pass to introduce a high density of dislocations, in combination with a long reheating interval to permit rearrangement, constitutes the most suitable TMP for the development of a microstructure capable of sustaining superplastic deformation mechanisms in this material.

4. *Rolling temperature (TMP V: 220 °C vs 300 °C vs 350 °C)*

The role of recovery during processing on the resultant mechanical behavior was addressed further by selecting two additional temperatures, one above (350 °C) and the other below (220 °C) the usual rolling temperature (300 °C). The results are illustrated in Figure 3(d). Increasing the rolling temperature from 220 °C to 350 °C results in both reduced flow stress and increased m value at strain rates of $\approx 10^{-3}$ s^{-1}, and the corresponding ductility rises from ≈200 pct to ≈350 pct. From this, it is apparent that recovery processes and precipitation reactions during the TMP are as important as the magnitude of the dislocation density when selecting process variables for optimum superplastic response. Also, the rolling temperature must remain below the β-phase solvus temperature. Brief static annealing above the solvus results in dissolution of the β phase and rapid microstructural coarsening with diminished ductility during subsequent deformation at 300 °C.[10] It should be noted that increasing the reheating time to 30 minutes during rolling at 300 °C (TMP IV or TMP VI) produced a larger improvement in ductility than increasing the rolling temperature to 350 °C.

B. *Texture Analysis*

The pole figure data in Figures 4(a) through (c) reflect the changes in texture which occur for the TMP III material from (*a*) the as-rolled condition, (*b*) during static annealing, and (*c*) during superplastic deformation. The texture of the as-rolled condition may be approximated by the (112) [1$\bar{1}$1] ideal orientation (copper texture component). The (110) [1$\bar{1}$2] ideal orientation (brass texture component), which is considered to be a stable rolling texture component in many cold-rolled face-centered cubic alloys,[20] is not apparent in the texture resulting from TMP III. The scatter about the mean orientation in Figure 4(a) reflects both a distribution of grain orientations and lattice curvature due to the high matrix dislocation density remaining at the conclusion of rolling.

Heating to the testing temperature is the equivalent of a 1-hour static anneal at 300 °C, and following this, the texture has sharpened considerably. In Figure 4(b), both the {111} and {200} pole figures exhibit increased peak

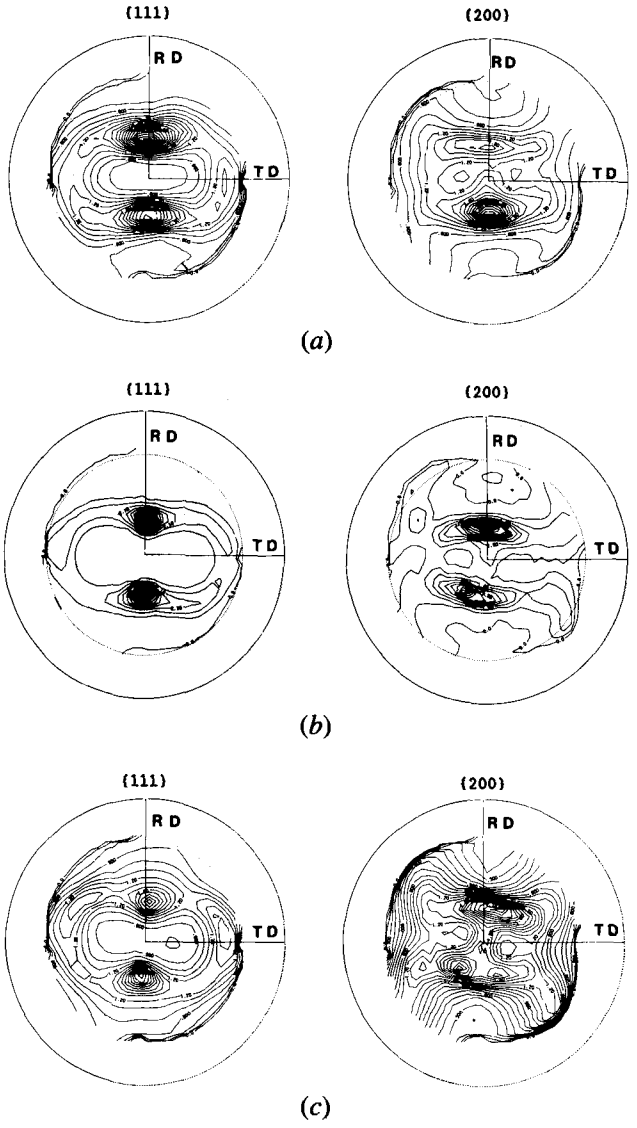

Fig. 4—Texture data for the TMP III material represented as {111} and {200} pole figures out to ≈70 deg to the sheet normal. The data indicate changes in texture from (*a*) the as-rolled condition, (*b*) after static annealing, and (*c*) after superplastic deformation.

intensities compared to the as-rolled condition, and no new orientations have appeared. Thus, it is likely that only recovery and polygonization reactions are responsible for the changes observed.[15,16] The texture sharpening is the result of a reduction in the density of matrix dislocations through mutual annihilation or migration to subboundaries. A similar effect has been reported in Al-Cu-Zr alloys and has been interpreted as evidence that the lattice curvature created by deformation processing becomes localized at boundaries of average boundary misorientation of ≈5 deg.[5,6]

After deformation to an elongation of 100 pct, it can be seen that the texture has been weakened. In Figure 4(c), no new texture components have emerged, and this is evidence that recrystallization involving nucleation and boundary migration has not occurred. However, this material is superplastic, with $m \approx 0.5$ at the onset of deformation, and thus, it can be assumed that a fine-grained microstructure is present in a large proportion of the material. Static continuous recrystallization results only in small changes in texture in association with recovery processes. However, during superplastic deformation, boundary misorientations will increase due to grain rotation associated with accommodation of the deformation mechanism. It may be surmised that grain rotation, possibly in conjunction with further (dynamic) continuous recrystallization, is responsible for the texture weakening observed here.

C. *Microstructural Investigations*

Transmission electron microscopy was used to assess the effect of the TMP variables on microstructure by measurement of the (sub)grain size. Grip sections represent the microstructural condition of the material after the completion of processing and subsequent preheating prior to deformation. Gage sections represent the condition of the microstructure at the completion of superplastic deformation at the strain rate which produced the peak ductility. In a previous study, the effect of rolling strain on (sub)grain size was small.[19] For this reason, only material which had been processed to a total rolling strain of ≈2.5 was evaluated here. The results, summarized in Table III, indicate no significant difference in the (sub)grain size in the grip sections for the different TMP schemes conducted at 300 °C. As reflected by the data for the corresponding gage sections, the extent of coarsening resulting from superplastic deformation becomes greater with increasing strain to failure.

The mean linear intercept (MLI) method was used to determine the (sub)grain size according to $d = 1.773\lambda$, where d is the grain size and λ is the mean linear intercept determined from micrographs.[21] There is inherent error in this technique for evaluating grain size here due to the uncertain nature of the boundaries being included in the analysis. It is important to note that during the acquisition of this data, no attempt was made to distinguish between low and high-angle boundaries. Even though the changes in grain size have been shown to be relatively small, there is an apparent correlation between the extent of microstructural coarsening and the peak ductility values. The microstructure in the TMP VI material, which had a strain-to-failure of 600 pct, coarsened to a greater extent than the TMP V (at 220 °C) material, which had a strain-to-failure of only 200 pct.

Microstructures representative of material in the various processed conditions and at the onset (grip sections) and the completion (gage sections) of superplastic deformation are presented in Figures 5 through 7. A

Table III. Mean Linear Intercept Data

TMP Schedule (ε_R = 2.5)	Specimen Location		Elongation at 10^{-3} s^{-1} (Pct)
	Grip (μm)	Gage (μm)	
III (300 °C)	1.9	2.3	375
IV (300 °C)	1.8	2.5	450
V (220 °C)	1.3	1.4	200
V (300 °C)	1.7	1.8	250
VI (300 °C)	2.0	2.4	600

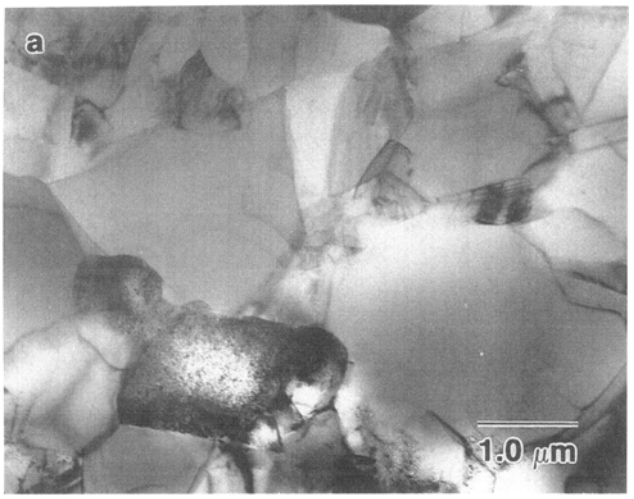

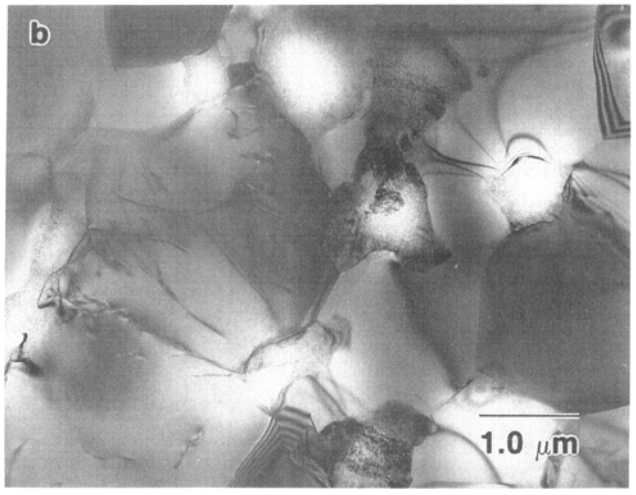

Fig. 5—The microstructure of the alloy in the TMP III condition in (*a*) the grip section, is seen to be slightly finer (1.9 μm) than in (*b*) the deformed gage section (2.3 μm).

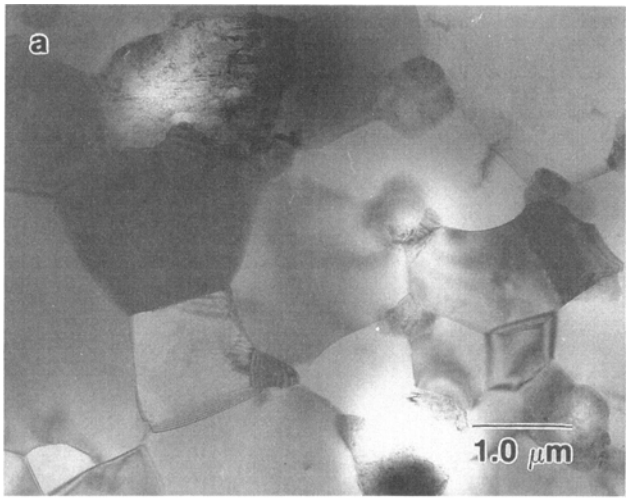

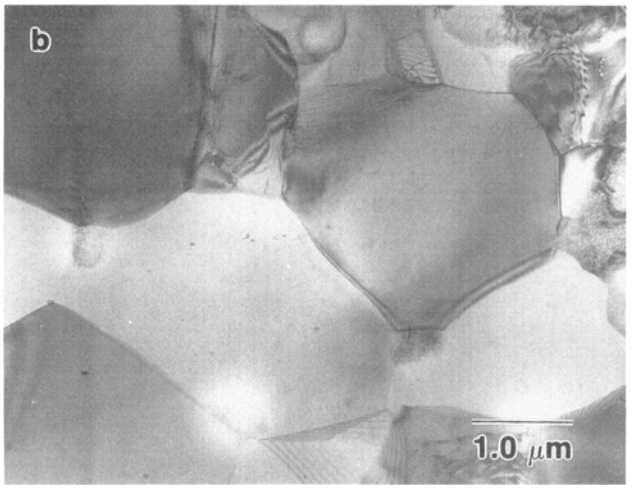

Fig. 6—The microstructures of the alloy in the grip section in (*a*) the TMP IV condition (1.8 μm), and (*b*) the TMP VI condition (2.0 μm).

comparison reveals that, as with the subtle variations detected by the mean linear intercept measurements, there is little apparent difference among the micrographs. In all cases, the materials exhibit a uniform, equiaxed microstructure with well-defined boundaries and a marked absence of matrix dislocations. The β phase apparently has precipitated in a preferential manner at structural triple junctions as relatively coarse ($\approx$0.5 μm) particles. Also, the heavily faulted precipitates have not coarsened appreciably during deformation and have maintained an irregular, polygonal shape.

IV. DISCUSSION: THE MICROSTRUCTURAL RESULTS

Qualitative information regarding the nature of the observed boundaries may be obtained from the microstructural data. It has been suggested that the presence of extinction contours at boundaries is indicative of a lack of internal strain.[22] Low-angle boundaries ($\Theta \leq 5$ deg) consist of regular arrays of individual dislocations, each with an associated stress field. As the boundary misorientation increases, the dislocations become more closely spaced and the extent of the overall stress field associated with the boundary decreases.[23] Thus, it may be assumed that only high-angle boundaries ($\Theta \geq 15$ deg), in which dislocations have lost their individual nature and, hence, their associated stress fields, exhibit extinction contours.[24] It should be noted that the information that can be obtained in this manner is strictly limited, since the presence of contours is a strong function of the TEM imaging conditions.

On this basis, reexamination of the micrographs in Figures 6(a) and (b) reveals that the TMP IV material, which exhibited lower ductilities, also shows less evidence of extinction contours (a) than is the case for the TMP VI material (b). Thus, the TMP VI material, which was processed with a reheating time of 30 minutes, has a slightly coarser microstructure but contains boundaries of greater misorientation compared with the TMP IV material, which has experienced the 4-minute reheating time. Likewise, the TMP III material, which shows no evidence of extinction contours in the grip section

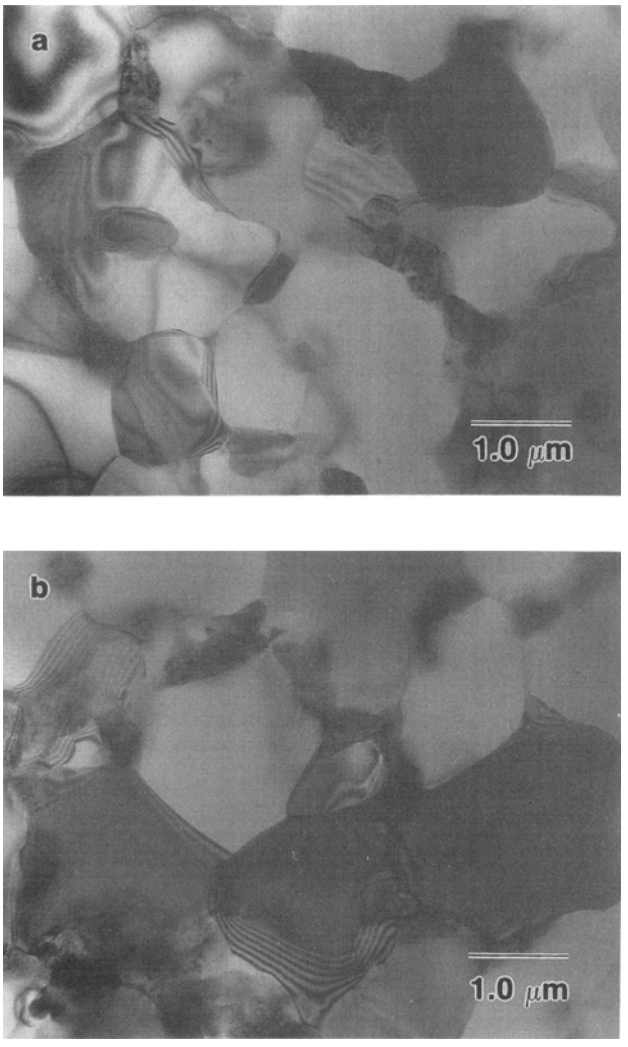

Fig. 7—The microstructures of the alloy in the TMP V condition after rolling at (*a*) 220 °C (1.4 μm) and (*b*) 300 °C (1.8 μm).

(Figure 5(a)) does exhibit some extinction contours following deformation, as seen in the gage section (Figure 5(b)). This is consistent with previous observations that there are substantial increases in boundary misorientations accompanying superplastic deformation of TMP III material.[10] Similarly, the gage sections for TMP V material, as seen in Figures 7(a) and (b) for both rolling temperatures, show contours but to a lesser extent than the other process conditions, and this material exhibited the low ductility. Thus, variations in the TMP affect both the nature of the boundaries as well as the grain size, and differences observed in mechanical behavior may be correlated with the nature of the boundaries in the microstructure.

The results of previously conducted misorientation studies using convergent beam electron diffraction techniques are summarized in Table IV for TMP V and TMP VI material.[12] The materials were annealed briefly (4 minutes) following the final rolling pass to reduce matrix distortion and to facilitate analysis using this method.[12] The more ductile TMP VI material exhibited a coarser structure but contained predominantly high-angle

Table IV. Boundary Misorientation Data

Type of Boundary	TMP V	TMP VI
Low-angle:		
(Θ < 15 deg)	71 pct	11 pct
High-angle:		
Coincident site lattice	10 pct	22 pct
Random	19 pct	67 pct

($\Theta \geq 15$ deg) boundaries. In contrast, the less ductile TMP V material contained predominantly low-angle ($\Theta < 15$ deg) boundaries. The cutoff value $\Theta = 15$ deg was chosen, in keeping with recent assessment of the role of boundaries in recrystallization.[25] During subsequent tensile deformation, not all of the boundaries present may be able to support grain-boundary sliding from the onset of deformation. But, providing that sufficient boundaries are capable of sliding, it is postulated that grain-boundary sliding can be the rate-controlling deformation mechanism. As a result, refined microstructures consisting of predominantly moderate angle boundaries may deform with m values of ≈ 0.5.

It is generally recognized that a refined grain structure, consisting of high-angle boundaries, is necessary for a material to exhibit superplasticity,[26,27] and for this reason, fine subgrain structures would not be satisfactory. In the Al-Cu-Zr alloys discussed earlier, the development of a well-defined substructure during the initial heating following TMP is a prerequisite for dynamic CRX during subsequent tensile deformation.[17] Subgrain coalescence is often cited as the primary mechanism of dynamic CRX. By this process, initially the lowest angle boundaries are eliminated through emission of dislocations followed subsequently by the elimination of boundaries progressively higher in misorientation.[28] The net result is a decrease in the number of boundaries and an increase in misorientation of the remaining boundaries by addition of dislocations.[29] The progressive nature of such processes makes it difficult to distinguish the point when substructures become grain structures.[30–34]

V. A MODEL FOR TMP-INDUCED CRX

The results of this work suggest the existence of an optimum TMP schedule to achieve a refined microstructure best suited for superplasticity. The objective here is to describe the conditions necessary to achieve a substructure which will readily undergo the reactions illustrated schematically in Figure 1. The desirable features of the substructure are well-defined subgrains stabilized by particles so that a high density of dislocations in subboundary walls may be attained. This circumstance will be superior to a very high but diffuse dislocation density with only a few random sites suitable for nucleation. It is proposed that, as such a refined substructure is progressively converted into a fine-grained microstructure during processing, the net process constitutes CRX.

The effect of using 30-minute reheating intervals between passes of 10 pct nominal reduction is to facilitate static recovery processes starting with the initial cycle. As illustrated in Figure 8, it is presumed that there is

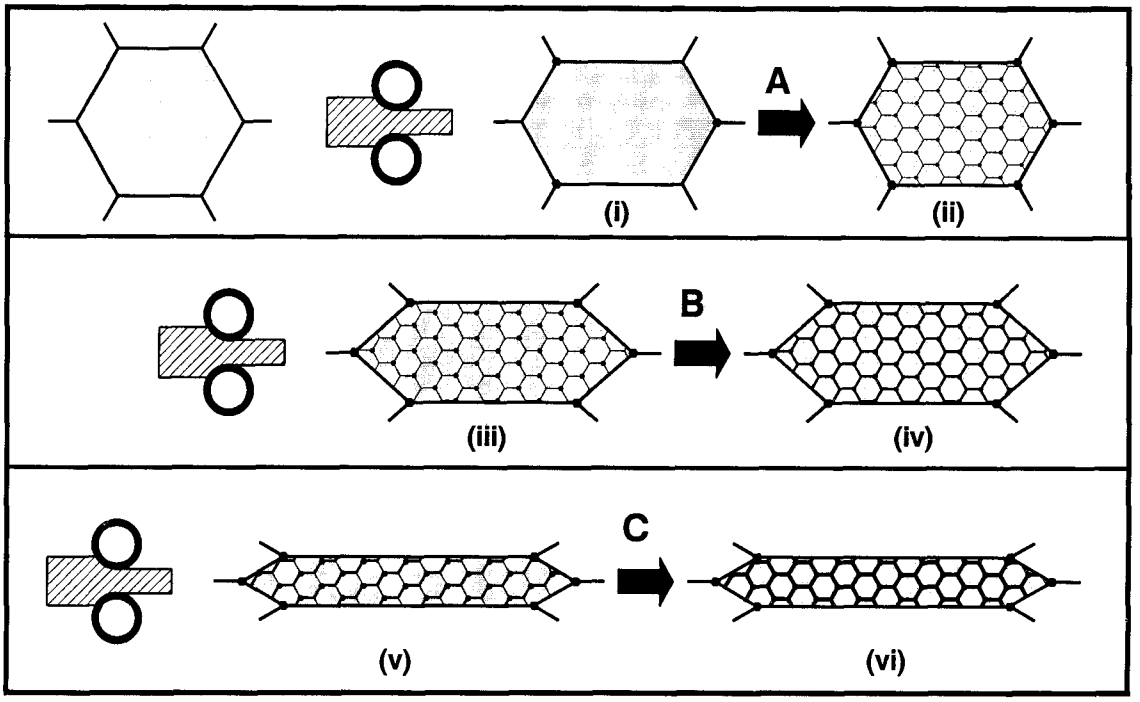

Fig. 8—A schematic representation of microstructural evolution through a sequence of rolling passes with reheating intervals of 30 min duration at 300 °C. Following the initial pass, reheating (A) results in the initiation of substructure development. Reheating intervals (B and C), after an intermediate pass and the penultimate pass, respectively, allow for a continued buildup in boundary misorientation as dislocations are incorporated into the subboundary walls. Precipitation of the β phase stabilizes the evolving structure.

adequate time for subgrain formation and enlargement during reheating, A, after the first rolling pass and that precipitation commences on the nodes of the substructure (ii). In subsequent passes, a high dislocation density again results (iii), and during the following annealing cycles, B, recovery of some of the dislocations generated to the preexisting subboundaries takes place (iv). As processing continues to completion, there will be a buildup of misorientation (vi) through the repeated cycles of rolling deformation (v) and static annealing intervals, C, assuming that precipitated particles retard the moving apart of dislocations within the arrays which constitute the boundaries. In this manner, a large proportion of the dislocations generated will be incorporated into the initially established subboundaries, thereby reducing the effective dislocation spacing in the boundaries. In turn, this will raise the misorientation and facilitate conversion to grain boundaries.

The microstructural changes occurring during 4-minute reheating intervals between rolling passes are shown schematically in Figure 9. The initial rolling pass will generate the same high dislocation density (i) and as depicted in Figure 8 (i). However, the 4-minute anneal, A, provides insufficient time for a well-defined substructure to develop, and there is only a reduction in dislocation density (ii). Precipitation barely commences and is very diffuse in the absence of a well-defined substructure. Following a later pass (iii), a high dislocation density is again present. Again with 4 minutes of annealing, B, recovery processes eliminate many internal dislocations but result only in minimal buildup of subboundaries (iv). Also, precipitation is not as effective in stabilizing the evolving structure. As a result of the entire schedule, a subgrain structure (vi) evolves which is smaller but more diffuse and less stabilized and with boundaries of lower misorientation than resulted with 30 minutes of annealing.

The evolution of the microstructure through cycles of deformation and annealing is also reflected in the resistance of the material to warm rolling. The flow stress increases with strain during the initial pass and decreases as recovery takes place in the ensuing reheating interval. As illustrated in Figure 10(a), the 30-minute reheating interval produces a greater extent of recovery. A gradual increase in the flow stress envelope over several cycles of straining and annealing is likely and, in the absence of strengthening due to precipitation of the β phase, would reach a plateau lower than the flow stress for continuous deformation as a result of the static recovery. However, the precipitation of the β phase stabilizes the substructure so that much higher dislocation densities, and hence, maximum flow stress values, can be attained compared to continuous deformation.

The extent of softening is more limited with 4-minute reheating intervals between rolling passes so that the flow stress envelope lies closer to the continuous curve as a result of a finer, more diffuse substructure compared to that produced with 30-minute reheating intervals. As a result of the decrease in overall time at temperature, precipitation of the β phase will also not be complete until a larger rolling strain is attained. During the early part of the schedule, there will be fewer β-phase precipitates present for stabilization so that the evolving substructure is less well-defined. Continuous deformation at the same temperature would result inherently in more extensive

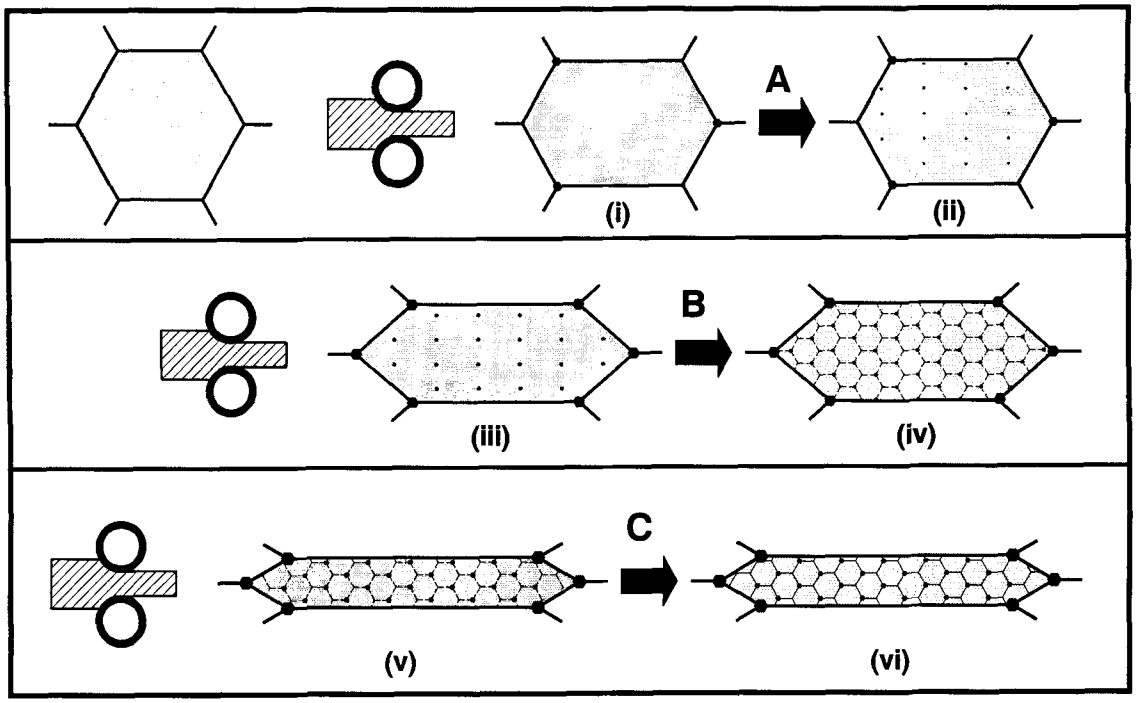

Fig. 9—Schematic representation of microstructural evolution through a sequence of rolling passes with reheating intervals of 4 min duration. Reheating (A) following the initial pass is insufficient for substructure formation. Reheating intervals (B and C) after subsequent passes allow for a gradual development of a subgrain structure with smaller cells having a lower wall density but higher interior density of dislocations than in Fig. 8. In comparison with Fig. 8, only the length of the reheating interval has changed.

hardening through an even finer and more diffuse substructure, with some strengthening due to precipitation of fine β phase concurrent with substructure formation.

The influence of rolling temperature with 4-minute reheating intervals is illustrated schematically in Figure 10(b). At lower rolling temperatures (220 °C), recovery and precipitation are much slower, which leads to a finer substructure characterized by boundaries which are more diffuse in nature.[15,16] Such a microstructure will not support superplastic deformation mechanisms.[25,26] At 350 °C, the development of a well-defined subgrain structure occurs more readily. However, the volume fraction and number of β-phase precipitates will be reduced, leading ultimately to a coarser microstructure.

Several features of this model deserve further attention. The strain in each rolling pass should be sufficient to produce a cellular substructure in order to ensure formation of subgrain boundaries during the subsequent reheating. The interval duration should permit recovery to progress through annihilation and rearrangement onward into coalescence and amalgamation *via* subgrain boundary migration. This will result in enlargement of the subgrains but also will leave the walls more regular and dense.[35,36] The reheating time must also permit sufficient β-phase precipitation on substructure nodes. The microstructure at the end of each reheating interval will thus be stable enough that it does not disintegrate in the dislocation flux of the next pass and, instead, will be able to serve as the framework for later dislocation interactions.[37] In each successive annealing stage, the newly introduced dislocations interact with each other and with the preexisting subgrain boundaries. This reduces the dislocation density in subgrain interiors as some of the dislocations integrate into existing arrays, thereby augmenting their misorientation and stability.

The precipitation of the β phase is an integral part of this process, since it may form heterogeneously on single dislocations or preferentially on networks.[14] Thus, a well-defined substructure will give rise to fewer but more stable particles which reside at nodes. Once formed, the particles stabilize the substructure by restricting the tendency of the dislocations within the subboundary walls to move apart. As the boundaries persist through many cycles of deformation and annealing, they will increase in stability and misorientation. On one side of optimum processing conditions, *e.g.*, too little strain, too short a time, or too low a temperature, the result is a diffuse dislocation structure with insufficient particle stabilization. On the other hand, too long a time or too high a temperature gives rise to widely dispersed, large particles and coarse subgrains with boundaries of low density and misorientation.

Concurrent deformation accelerates CRX by a factor of 10^2 to 10^3[13,14] by assisting the conversion of subgrain boundaries, where individual dislocations may be resolved, into grain boundaries, where dislocations have lost their identity. During the elevated temperature deformation stages of the TMP, shear stresses result in dislocation motion and in boundary sliding accompanied by some grain rotation. In the initial stages of processing, sliding would happen only on the original grain boundaries. As the microstructure evolves, sliding may begin to occur on boundaries as they reach $\approx$7 deg misorientation.[38] As this may arise randomly throughout the

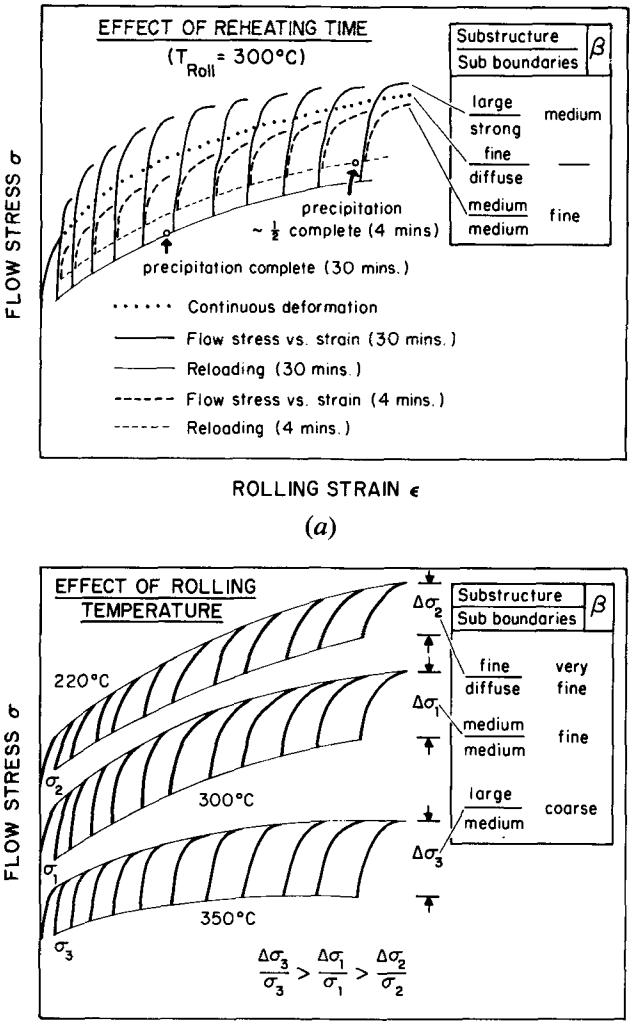

Fig. 10—The effect of (*a*) reheating time and (*b*) rolling temperature on the resistance of the material to straining during rolling. Both increased reheating interval and higher temperature lead to greater softening between rolling passes as a result of recovery. With a balance between deformation, recovery, and precipitation, a refined structure of moderate-angle grain boundaries may be achieved.

material, high misorientation subboundaries are progressively converted into grain boundaries. Since static CRX likely would require much greater times than afforded by the TMP, it is postulated that this conversion takes place in the final rolling passes. Such a process is unlikely during continuous deformation, because dynamic recovery would maintain subboundaries at a lower dislocation density.[15,16] At the lower deformation rates of superplastic flow, sliding will predominate and accelerate this progressive conversion of the subboundaries,[1,17] but only if prior processing has supplied enough sufficiently misoriented boundaries.

VI. CONCLUSIONS

1. The texture and microscopy data demonstrate that recrystallization by nucleation and boundary migration does not occur during TMP of this Al-Mg-Zr alloy. However, the mechanical property data show that the resultant structure is capable of sustaining a superplastic response from the onset of straining with a sufficient balance between deformation and recovery during the processing.
2. Existing concepts of static and dynamic CRX have been combined to describe the progressive conversion of a heavily deformed condition into a refined grain structure. Static and dynamic recovery of dislocations to a particle-stabilized substructure leads to a fine-grained microstructure during repeated cycles of deformation and annealing at 300 °C. The β-phase precipitates stabilize the substructure, and this leads to the development by CRX of a grain size on the order of the interparticle spacing.
3. The complex sequence occurring during TMP includes as central features the following:
   a. processing temperature, strain per pass, and reheating interval, permitting sufficient recovery to form well-defined subboundaries;
   b. dislocation accumulation in boundaries whose recovery or migration is restricted by the precipitation of β phase at triple junctions;
   c. boundary dislocation density increase such that misorientations develop sufficiently to facilitate conversion into grain boundaries.
4. Enhanced superplastic response in this alloy is obtained by selection of thermomechanical processing variables to induce the generation of well-defined subgrains so stabilized by β particles that the boundary dislocation density promotes dynamic CRX.

ACKNOWLEDGMENTS

This research has been supported by the Naval Air Systems Command with Dr. Lewis Sloter as program monitor. The acquisition and reduction of the MLI data by Dr. Ahmed Salama at the Naval Postgraduate School and the pole figure data by Dr. Wolfgang Ruch at the University of Virginia is gratefully acknowledged. Assistance in preparation of the schematic figures by Mr. Robert Hafley is also much appreciated.

REFERENCES

1. B.M. Watts, M.J. Stowell, B.L. Baikie, and D.G.E. Owen: *Met. Sci.*, 1976, vol. 10, pp. 189-97 and 198-205.
2. E. Nes: *Mater. Sci.*, 1978, vol. 13, pp. 2052-55.
3. E. Nes: *Met. Sci.*, 1979, vol. 13, pp. 211-20.
4. R.H. Bricknell and J.W. Edington: *Metall. Trans. A*, 1979, vol. 10A, pp. 1257-63.
5. R.H. Bricknell and J.W. Edington: *Acta Metall.*, 1979, vol. 27, pp. 1303-11.
6. E. Nes: in *Superplasticity*, B. Baudelet and M. Suery, eds., Centre National de la Recherche Scientifique, Paris, 1985, pp. 7.1-7.14.
7. T.R. McNelley, E.-W. Lee, and M.E. Mills: *Metall. Trans. A*, 1986, vol. 17A, pp. 1035-41.
8. E.-W. Lee, T.R. McNelley, and A.F. Stengel: *Metall. Trans. A*, 1986, vol. 17A, pp. 1043-50.
9. E.-W. Lee and T.R. McNelley: *Mater. Sci. Eng.*, 1987, vol. 93, pp. 45-55.
10. S.J. Hales and T.R. McNelley: *Acta Metall.*, 1988, vol. 36, pp. 1229-39.

11. S.J. Hales and T.R. McNelley: in *Superplasticity in Aerospace*, H.C. Heikkenen and T.R. McNelley, eds., TMS-AIME, Warrendale, PA, 1988, pp. 61-76.
12. R. Crooks, S.J. Hales, and T.R. NcNelley: in *Superplasticity and Superplastic Forming*, C.H. Hamilton and N.E. Paton, eds., TMS-AIME, Warrendale, PA, 1988, pp. 389-93.
13. E. Hornbogen and U. Köster: in *Recrystallization of Metallic Materials*, 2nd ed., F. Haeßner, ed., Riederer-Verlag, Stuttgart, Federal Republic of Germany, 1978, pp. 159-94.
14. E. Hornbogen: *Metall. Trans. A*, 1979, vol. 10A, pp. 947-72.
15. H.J. McQueen and J.J. Jonas: *Treatise on Materials Science and Technology*, Academic Press, New York, NY, 1975, vol. 6, pp. 393-493.
16. H.J. McQueen and K. Conrod: in *Microstructural Control in Aluminum Alloys: Deformation, Recovery and Recrystallization*, E.H. Chia and H.J. McQueen, eds., TMS-AIME, Warrendale, PA, 1986, pp. 197-219.
17. R.A. Ricks and P.-J. Winkler: in *Superplasticity and Superplastic Forming*, C.H. Hamilton and N.E. Paton, eds., TMS-AIME, Warrendale, PA, 1988, pp. 377-81.
18. L.F. Mondolfo: *Aluminum Alloys—Structure and Properties*, Butterworth's, London, 1979, pp. 311-23.
19. S.J. Hales, S.B. Oster, B.W. Sanchez, and T.R. McNelley: *J. Phys.*, 1987, vol. 48, pp. 285-91.
20. C.S. Barrett and T.B. Massalski: *Structure of Metals*, 3rd ed., McGraw-Hill, New York, NY, 1966, pp. 541-67.
21. G.F. Vander Voort: *Metallography—Principles and Practice*, McGraw-Hill, New York, NY, 1984, p. 449.
22. R.D. Heidenreich: *J. Appl. Phys.*, 1949, vol. 20, pp. 943-54.
23. J.P. Hirth and J. Lothe: *Theory of Dislocations*, McGraw-Hill, New York, NY, 1968, pp. 669-72.
24. H. Hu: *Trans. TMS-AIME*, 1964, vol. 230, pp. 572-80.
25. R.D. Doherty, G. Gottstein, J. Hirsch, W.B. Hutchinson, K. Lucke, E. Nes, and P.J. Wilbrandt: *Proc. 8th Int. Conf. on Textures in Materials (ICOTOM 8)*, J.S. Kallend and G. Gottstein, eds., TMS-AIME, Warrendale, PA, 1988, pp. 563-72.
26. O.D. Sherby and P.M. Burke: in *Progress in Materials Science*, B. Chalmers and W. Hume Rothery, eds., Pergamon Press, Oxford, United Kingdom, 1968, vol. 13, pp. 325-90.
27. T.H. Alden: in *Treatise on Materials Science and Technology*, R.J. Arsenault, ed., Academic Press, New York, NY, 1975, vol. 6, pp. 225-66.
28. K. Lintermanns and H.A. Kuhn: in *Aluminum Alloys—Their Physical and Mechanical Properties*, E.A. Starke and T.H. Sanders, eds., Chameleon Press, London, 1986, pp. 529-43.
29. H.J. McQueen: *Mater. Sci. Eng.*, 1988, vol. A101, pp. 149-60.
30. M.A. Zaidi and T. Sheppard: *Met. Sci.*, 1982, vol. 16, pp. 229-38.
31. N. Raghunathan, M.A. Zaidi, and T. Sheppard: *Mater. Sci. Technol.*, 1986, vol. 2, pp. 938-45.
32. R.A. Varin: *Mater. Sci. Eng.*, 1984, vol. 66, pp. 97-103.
33. R.A. Varin and K. Tangri: *Z. Metallkd.*, 1982, vol. 73, pp. 144-48.
34. J.K. Solberg, H.J. McQueen, N. Ryum, and E. Nes: *Phil. Mag.*, 1989, vol. 60, pp. 447-71.
35. H.J. McQueen and E. Evangelista: *Czech. J. Phys.*, 1988, vol. B38, pp. 359-72.
36. T. Hasegawa, T. Yakou, and U.F. Kocks: *Acta Metall.*, 1982, vol. 30, pp. 235-43.
37. H.J. McQueen, E.H. Chia, and E.A. Starke: in *Microstructural Control in Aluminum Alloys—Deformation, Recovery and Recrystallization*, E.H. Chia and E.A. Starke, eds., TMS-AIME, Warrendale, PA, 1986, pp. 1-18.
38. F. Weinberg: *Trans. TMS-AIME*, 1958, vol. 212, pp. 808-17.